Transporting Heat Flux From the US and Europe to Antarctica Guided by Regional Seismic Structure

Shane Zhang[*1] and *Michael H. Ritzwoller*[1]

[1] Department of Physics, University of Colorado Boulder, Boulder, CO 80309, USA.

Abstract

Subglacial geothermal heat flux affects the dynamics of the Antarctic ice sheet but is poorly known. We estimate heat flux across West Antarctica and the interior of East Antarctica by transporting heat flux observations from the contiguous US and Europe, based on seismic structure with a lateral resolution of about 100 km. We transport with three Machine Learning models across a hierarchy of complexity (Linear Regression, Decision Tree, and Random Forest). We have validated the models within the US and Europe and cross-validated them between the two continents. The uppermost mantle shear wavespeed is the primary predictor. The geographical patterns can be reasonably reproduced but the variability tends to be underestimated. Antarctic heat flux estimates are highly consistent between the three Machine Learning models, but we report the Decision Tree results. In West and East Antarctica, respectively, we estimate subcontinental-scale heat flux values of $64 \pm 7\,\mathrm{mW/m^2}$ (spatial mean $\pm$ standard deviation) and $53 \pm 3\,\mathrm{mW/m^2}$. Heat flux varies regionally across West Antarctica from $50\,\mathrm{mW/m^2}$ to $83\,\mathrm{mW/m^2}$ and across East Antarctica from $50\,\mathrm{mW/m^2}$ to $74\,\mathrm{mW/m^2}$. Particularly high heat flux occurs in the western Transantarctic Mountains and Marie Byrd Land in West Antarctica and the lowest heat flux occurs in Victoria Land, the Wilkes Subglacial Basin, the Vostok Subglacial Highland, and south of Maud Subglacial Basin in East Antarctica. We estimate systematic errors including a constant shift in the continental average ($2.5\,\mathrm{mW/m^2}$) and a variability (higher highs, lower lows) of 25% from the continental average, along with an average random error of about $13\,\mathrm{mW/m^2}$ in West Antarctica and $10\,\mathrm{mW/m^2}$ in East Antarctica. Our estimates are consistent with a recent seismically-based study by Shen, Wiens, Lloyd, and Nyblade [1] but are significantly lower in West Antarctica than a magnetically-based study by Martos et al. [2]. To resolve such inconsistencies, validation of all proxies against heat flux observations outside Antarctica is needed.

Contents

1 Introduction **3**

1.1 Motivation 3

1.2 Problem statement 3

*shane.zhang@colorado.edu

1.3 Previous studies . . . 3
1.4 Methodology . . . 4
1.5 Outline . . . 4

2 Data **4**
2.1 Geothermal heat flux observations . . . 5
2.2 Seismic structure . . . 5

3 Methods **6**
3.1 Machine Learning models . . . 6
3.2 Validation within and cross-validation between the US and Europe . . . 6
3.3 Transporting heat flux to Antarctica . . . 7
3.4 Uncertainty estimation . . . 7

4 Results **8**
4.1 Heat flux dichotomy between East and West Antarctica . . . 8
4.2 Regional heat flux anomalies across Antarctica . . . 8
4.3 Source regions of Antarctic heat flux anomalies in the US and Europe . . . 9

5 Discussion: Comparison with Previous Studies **9**

6 Conclusion **11**

Figures **13**

Acknowledgements **18**

A Decision rules **19**

B Uncertainty estimation **20**

References **25**

List of Figures

1 Heat flux observations. . . . 13
2 Seismic structure. . . . 14
3 Heat flux predictions across Antarctica. . . . 15
4 Identifying regions in the US and Europe that transport heat flux to Antarctica. 16
5 Comparison with previous studies. . . . 17
A.1 Decision rules obatined from the Decision Tree model. . . . 19
B.1 Sources of uncertainties. . . . 22
B.2 Uncertainty versus heat flux. . . . 23
B.3 Differences between predictions from the three Machine Learning models. . . . 24

1 Introduction

1.1 Motivation

Geothermal heat flux is the amount of heat per unit time per unit area ($\mathrm{J\,s^{-1}\,m^{-2}}$) transported from the interior of the solid Earth to the Earth's surface, which in Antarctica is principally the ice-bedrock interface. Heat flux is a part of the lower boundary conditions for ice sheets and can influence their thermomechanical state by weakening basal ice and inducing subglacial melt and glacial erosion [3–9]. This can accentuate ice flow and Antarctica's contribution to future sea level change [10–15]. Improved understanding of subglacial heat flux would illuminate the dynamics of the Earth's climate system to improve predictions of future climate change [16].

Direct observations of heat flux beneath the Antarctic ice sheet, however, remain rare because of the difficulty and expense of drilling to acquire measurements [17, 18]. Subglacial heat flux, therefore, introduces a significant uncertainty into Antarctic ice sheet models [6, 16]. As a consequence, indirect estimates of Antarctic geothermal heat fluxn based on various proxies have attracted much recent interest over the past two decades [1, 2, 19–34]. There remain, however, significant discrepancies amongst Antarctic heat flux estimates inferred from different proxies [17].

1.2 Problem statement

We aim to provide reliable estimates of Antarctic heat flux on both continental and regional scales based on a validated methodology.

First, across the continent of Antarctica, we seek to determine the mean and spatial variability of heat flux for West and East Antarctica. We refer to this as the continental *dichotomy* problem. The amplitude of the dichotomy derives from the fundamental difference between West and East Antarctica in tectonic and geologic histories. Reliable estimates on the continental scale can serve as a basis for further refinement of heat flux estimates.

Second, on a regional scale, we also seek to determine the highest and lowest heat flux values and where they are located. We call this the regional *anomaly* problem. The high and low heat flux anomalies can affect ice sheet dynamics on a regional scale. This is fundamental towards refining the spatial resolution of heat flux estimates to come closer to that of ice sheet models.

1.3 Previous studies

Inferences of Antarctic heat flux are largely made through different proxies, including seismic structure [1, 19], magnetic Curie depth [2, 28], and surface topography [26]. Here, we focus on seismic structure as a proxy because seismic inversion vertically resolves both the crust and uppermost mantle [35, 36]. Hence, seismic structure can relate heat flux with features at specific depths, while most other proxies cannot. Moreover, recent development in seismic instrumentation and methodology have improved the lateral resolution of estimates of Antarctic seismic structure to about 100 km [e.g., 37, 38], comparable to other continents.

Estimates of Antarctic heat flux inferred from different proxies are inconsistent [17]. One reason is that most studies that infer heat flux have not yet been subject to validation in which heat flux predictions are compared with observations where such observations exist. Such validation is crucial for evaluating the transportability of heat flux estimation methods from the regions where they are developed (where heat flux measurements may be plentiful) to Antarctica.

1.4 Methodology

To evaluate the transportability of heat flux measurements from outside Antarctica, our previous work used Machine Learning methods to relate seismic structure to heat flux in the contiguous US and Europe [39]. We compare three Machine Learning models across a hierarchy of complexity. These are Linear Regression, Decision Tree, and Random Forest models. We validated the models with holdout data within a continent and cross-validated them between the US and Europe, in which models developed in the US were applied in Europe and vice versa. Based on insights from this validation and cross-validation, in this paper we transport heat flux estimates to Antarctica from the US and Europe. We evaluate the reliability of Antarctic heat flux estimates by contrasting the predictions from the Machine Learning models, comparing the US versus Europe heat flux data, and propagating errors in seismic structure information and heat flux observations to estimate uncertainties in the estimated heat flux.

We note two terminological conventions in this paper. First, we refer to locations within Antarctica using the terms north, south, east, and west to mean grid-north, grid-south, grid-east, and grid-west, respectively, where the reference grid is defined by the Antarctic maps presented in **Figs 3** and **4**. Up is grid-north, right is grid-east, etc. Second, there are two types of "models" discussed herein. There are heat flux models that relate seismic structure to surface heat flux estimates. When we use the term model in this paper, this is what we mean. There are also 3-D models of seismic shear wave speed, which we refer to as seismic "structure" and do not use the term model to refer to them.

1.5 Outline

We first present heat flux data in the US and Europe and information about seismic structure in the US, Europe, and Antarctica (**section 2**). We then describe the Machine Learning models and insights gained from validation within and cross-validation between the US and Europe. These insights guide our estimates of heat flux with associated uncertainties for Antarctica (**section 3**). In **section 4**, we present our heat flux estimates across Antarctica and identify regions in the US and Europe that transport heat flux to Antarctica. We close by comparing our estimates with existing work (**section 5**).

2 Data

In this section, we describe the data sources and our processing of both heat flux observations (**section 2.1**) and seismic structure (**section 2.2**).

2.1 Geothermal heat flux observations

To estimate heat flux across Antarctica, we transport heat flux from the US and Europe because most continental heat flux observations are in those two continents. For both the US and Europe, our primary source of heat flux observations is the New Global Heat Flow (NGHF) database [40]. The NGHF database is complemented by the Southern Methodist University data in the central and Eastern US [41].

Due to the lack of information on the quality of the heat flux observations, we perform our own quality control. This involves data rejection and imputation based on data ranges, spatial variability, and non-steady state effects (e.g., hydrothermal circulations). Then, the data points are smoothed onto a map with a 50 km × 50 km grid. For each grid point, the median and MAD (median absolute deviation) are computed within a radius of 100 km. The gridded median heat flux values in the US and Europe are presented in **Fig. 1**. The MAD values measure spatial variability and are used as a proxy for errors in the median values (**section 3.4**).

2.2 Seismic structure

Information about seismic structure in the US, Europe, and Antarctica is from Shen and Ritzwoller [35], Lu, Stehly, and Paul [36], and Shen et al. [37], respectively. These structure estimates have a lateral resolution of about 100 km. This has improved significantly from previous global structure information with resolution worse than 300 km, which is used as a proxy for earlier estimates of Antarctic heat flux [e.g., 42]. This improvement benefits from the emergence of continental-scale seismic arrays and the innovations in methodology such as ambient noise tomography [e.g., 43, 44]. Moreover, structure information possesses uncertainty estimates determined from a Bayesian Monte Carlo approach [45].

To extract representative features from the seismic structures, we have identified three variables with a clustering analysis. These three seismic structural variables are the shear wavespeed V_S at 15 km depth (crust), V_S at 65 km depth (uppermost mantle), and Moho depth (**Fig. 2**). Moreover, we standardize each variable in each continent, because different seismic data and imaging methodologies are used on different continents [35–37]. To standardize variable x, we remove its spatial median μ and then divide by its interquartile range (IQR; range between the 25th and 75th percentiles) γ,

$$x' = \frac{x - \mu}{\gamma}. \tag{1}$$

For a Gaussian distribution, the IQR is larger than the standard deviation by a factor of about 1.35.

We then interpolate the three seismic structure variables onto the same 50 km × 50 km grid as heat flux data (**section 2.1**). Together with the heat flux maps, the seismic structure maps are the input to the Machine Learning models (**section 3.1**).

3 Methods

In this section, we first describe the Machine Learning models (**section 3.1**) and then summarize insights from validation within and cross-validation between the US and Europe (**section 3.2**). These insights are then applied to transporting heat flux to Antarctica (**section 3.3**) and estimating associated uncertainties (**section 3.4**).

3.1 Machine Learning models

We consider three Machine Learning models to relate seismic structure to surface (subglacial) heat flux, namely the Linear Regression, Decision Tree [e.g., 46], and Random Forest [47] models. These models span a hierarchy of complexity, where they model variations of the relationship between heat flux and seismic structure on the continental (Linear Regression), regional (Decision Tree), and local (Random Forest) scales, respectively [39].

3.2 Validation within and cross-validation between the US and Europe

The validation within and cross-validation between the US and Europe are our basis for transporting heat flux predictions to Antarctica [39].

In the validation process, we split the data within a continent (in the US alone or Europe alone) into a training dataset and a validation dataset. We then fit the Machine Learning models to the training dataset and evaluate model accuracy against the validation dataset. For both the US and Europe, we find that seismic structure can explain more than half of the observed heat flux variations. Uppermost mantle V_S is identified as the primary predictor of heat flux, with crustal V_S and Moho depth being secondary. However, crustal V_S and Moho depth are relatively more important for tectonically stable regions (e.g., Eastern US and Northeastern Europe).

During the cross-validation procedure, we evaluate model transportability by applying the US-trained models against the European data, and vice versa. For all three models, we find that the geographic patterns of heat flux are reasonably reproduced from one continent to the other. However, we find that the absolute amplitudes of variations are under-predicted in Europe when using the US models and over-predicted in the US when using the European models. Moreover, we find that the absolute amplitudes can be better predicted if heat flux observations are standardized in each continent (**eq.** (1)). Standardization shifts the median of the data across each continent to zero and divides the continental distribution by a measure of its spread. European heat flux data have a higher median value and greater spread than the US data. This standardization reduces the influence of these differences in the heat flux data between the two continents.

From the validation and cross-validation, we find that the Decision Tree and Random Forest models are the most accurate, while the Decision Tree and Linear Regression models are the most transportable. The Decision Tree model has what we see as a beneficial characteristic: it divides the whole area into several regions that are geologically relevant. For each region, it specifies a unique relationship between seismic structure and heat flux with a

decision rule. We find that the Random Forest model tends to overfit and produce variations with scales smaller than the resolution of seismic structure.

3.3 Transporting heat flux to Antarctica

To transport heat flux from the US and Europe to Antarctica, we first combine the US and European data. To combine the data, we separately standardize heat flux observations in each continent (**eq.** (1)). This is because our cross-validation shows that the absolute amplitudes of heat flux are better reproduced after standardization [39]. Then we combine these two standardized datasets by giving them equal weights. We discuss the effects of weights in **section 3.4**.

We then train the Machine Learning models with the combined data. In particular, the decision rules obtained from the Decision Tree model are discussed in **appendix A**. We apply the resulting models to the Antarctic seismic data to estimate heat flux across Antarctica. The estimates are smoothed using a Gaussian filter with a standard deviation of 50 km. This is because the seismic structure information has a resolution of about 100 km. To produce the final heat flux prediction, we undo the standardization of heat flux. This undoing involves multiplying the normalized heat flux prediction by a variation γ and then adding a median μ (**eq.** (1)). We apply the median and variation by weighing the US and European data equally ($\mu = 57\,\mathrm{mW/m^2}, \gamma = 19\,\mathrm{mW/m^2}$). This undoing has attendant uncertainties, which we discuss next (**section 3.4**).

3.4 Uncertainty estimation

We discuss uncertainty estimation in detail in **appendix B**, but summarize the results here. We identify and quantify four main sources of uncertainty in our heat flux estimates across Antarctica. The first two are systematic errors that may introduce a bias in the estimate and the latter two are non-systematic or random errors. First, we estimate a constant shift, ϵ_μ, caused by the difference in the continental average of heat flux observations between the US and Europe. We estimate its amplitude to be about $2.5\,\mathrm{mW/m^2}$. Second, we estimate an uncertainty in variability (higher highs, lower lows), ϵ_γ, caused by the difference in the continental variability of heat flux observations between the US and Europe. We estimate its amplitude to be $\epsilon_\gamma \approx 0.25|q - \mu|$ where q is a local heat flux estimate and μ denotes the spatial median of heat flux. Therefore, a heat flux estimate of $70\,\mathrm{mW/m^2}$ can have an uncertainty of about $2.5\,\mathrm{mW/m^2}$. Third, we estimate an uncertainty, ϵ_m, from the difference in the Machine Learning models trained in the US versus Europe. We estimate its amplitude to be about $3\,\mathrm{mW/m^2}$. Fourth, we estimate an uncertainty ϵ_v from uncertainties in seismic structure information in Antarctica, which is typically about $7\,\mathrm{mW/m^2}$ and is the largest among all errors. In contrast, we estimate the uncertainty to be small from errors in heat flux observations in the US and Europe, which is less than $1\,\mathrm{mW/m^2}$.

We estimate the final uncertainty ϵ by combining the four major uncertainties and assuming that they are independent from each other:

$$\epsilon = \underbrace{\pm\epsilon_\mu \pm \epsilon_\gamma}_{\text{systematic}} \underbrace{\pm\sqrt{\epsilon_m^2 + \epsilon_v^2}}_{\text{random}}. \tag{2}$$

The majority of the uncertainty is non-systematic (ϵ_m, ϵ_v), but the estimates have both a systematic bias ϵ_μ of about 2.5 mW/m^2, which is constant across the map, and systematic variability ϵ_γ of about 25% from the continental average. The combined uncertainties are presented in **Fig. 3**d–f. If an ensemble of heat flux estimates is to be derived from perturbing our estimates, however, the combined uncertainties should not be used. Instead, the systematic and random errors should be considered separately according to **eq.** (2).

4 Results

In this section, we discuss our predicted heat flux with associated uncertainties across West Antarctica and the interior of East Antarctica, focusing on the dichotomy between East and West Antarctica (**section 4.1**) and regional high or low heat flux anomalies (**section 4.2**). Then we identify structurally similar regions between Antarctica, the US, and Europe (**section 4.3**) to illuminate which regions of the US and Europe contribute to Antarctic heat flux predictions.

4.1 Heat flux dichotomy between East and West Antarctica

All three models delineate the West-East Antarctica dichotomy separated by the Tansantarctic Mountains. This dichotomy also appears in both the uppermost mantle V_S and Moho depth (**Fig. 2**hi). From the Decision Tree model, the spatial mean and standard deviation of heat flux values are 64 ± 7 mW/m^2 and 53 ± 3 mW/m^2 (mean $\pm$ standard deviation) for West and East Antarctica, respectively. These values are similar to those from the Linear Regression and Random Forest models.

Local uncertainties in our estimates of heat flux across West and East Antarctica are about 13 mW/m^2 and 10 mW/m^2 (spatial median), respectively, in the Decision Tree Model. Larger average uncertainties in West Antarctica derive mainly from the uncertainty in seismic structure ϵ_v (**section 3.4**). This is because heat flux values in West Antarctica are higher and more variable, and a small perturbation to the seismic structure can produce large changes in heat flux predictions.

4.2 Regional heat flux anomalies across Antarctica

From all three Machine Learning models, we identify two high heat flux anomalies (80 ± 20 mW/m^2) in West Antarctica (**Fig. 3**a–c). These are located in the western Transantarctic Mountains (Ellsworth, Whitmore, and Thiel Mountains) and Marie Byrd Land. These anomalies are associated with the very slow uppermost mantle V_S there (**Fig. 2**i). The rest of West Antarctica has relatively high heat flux (65 mW/m^2), which is associated with the relatively slow uppermost mantle V_S (**Fig. 2**i).

Based on the Linear Regression and Decision Tree models, we find the lowest heat flux values (50 ± 7 mW/m^2) near the periphery of our study region in East Antarctica (Victoria Land, Wilkes Subglacial Basin, Vostok Subglacial Highland, and south of Maud Subglacial Basin). These low values are associated with fast uppermost mantle V_S and thick crust. Intermediate heat flux values are found in the rest of East Antarctica (55 mW/m^2).

For all three models, heat flux is somewhat elevated in the Gamburtsev Subglacial Mountains from the rest of East Antarctica because of its relatively slow uppermost mantle V_S and deep Moho. In contrast, heat flux is depressed in the center of the Ross Ice Shelf from the rest of West Antarctica due to its fast uppermost mantle and crustal V_S (**Fig. 2**g–i). We also estimate relatively large uncertainties ($15\,mW/m^2$) at these two regions. This is because the crust is very thick in the Gamburtsev Subglacial Mountains and thin in the Ross Ice Shelf, and the Moho depth plays a different role between the US and European models [39].

4.3 Source regions of Antarctic heat flux anomalies in the US and Europe

Based on the Decision Tree model, we compare regions with similar seismic structure between Antarctica, the US, and Europe (**Fig. 4**). This illuminates where predictions derive in the Decision Tree model and shows the unique advantage of the Decision Tree model for geologically relevant regionalization.

On a subcontinental scale, West Antarctica has high heat flux because it has seismic structure similar to both the Alps in Europe, and the Colorado Plateau and Columbia River region in the US. These regions are characterized by the relatively slow uppermost mantle V_S and fast crustal V_S. On the other hand, East Antarctica has low heat flux because its seismic structure is similar to both the basins to the north of the Alps (North Germany Basin, Paris Basin, Ebro Basin) and the Apennines and Dinarides to the south of the Alps in Europe, and the Mississippi Embayment and Eastern Rocky Mountains in the US. These regions are characterized by relatively fast uppermost mantle V_S and either slow crustal V_S or thick crust.

On a regional scale, the western Transantarctic Mountains and Marie Byrd Land have the highest heat flux, which is transported from the Snake River Plain, the Basin and Range, and the Rio Grande Rift in the Western US, and the Pannonian Basin and Anatolia in Europe. These regions are characterized by a very slow uppermost mantle and crustal V_S. In contrast, the periphery of our study region in East Antarctica has the lowest heat flux, which is transported from both the Interior Plains in the central and Eastern US, and the Baltic Shield and Russian Platform in northwest Europe. These regions are characterized by a fast uppermost mantle and crustal V_S.

5 Discussion: Comparison with Previous Studies

We now compare our Antarctic heat flux estimates with the two recent studies of Shen, Wiens, Lloyd, and Nyblade [1] and Martos et al. [2]. Our estimates are similar for the Linear Regression and Decision Tree models, but we use Linear Regression estimates for comparison because the Decision Tree estimates are discrete and are less informative when compared visually to data. Martos et al. [2] estimates heat flux from thermal modeling based on the magnetic Curie depth, which they determine from airborne magnetic data. Shen, Wiens, Lloyd, and Nyblade [1] and our study both estimate heat flux based on seismic structure and the extraploation of heat flux observations from elsewhere in the world. However, Shen, Wiens, Lloyd, and Nyblade [1] use heat flux observations only from the US and consider a different Machine Learning model (k-nearest neighbors) similar to that of Shapiro and

Ritzwoller [19]. To the best of our knowledge, neither of the studies of Shen, Wiens, Lloyd, and Nyblade [1] and Martos et al. [2] were validated against observations elsewhere in the world. We focus the comparison on heat flux estimates of the largest scale, namely the continental dichotomy in these studies. We believe that a more refined comparison would be more informative after those studies were validated against observations.

In comparing the predictions from the different studies, it is important to use as a touchstone the distributions of heat flux observations in the US and Europe (**Fig. 5**ab). We believe it is unlikely that heat flux distributions in Antarctica will differ greatly from the US and Europe. We see Western US and Southwestern Europe as analogues of West Antarctica, as all have been recently deformed tectonically. We also believe the Eastern US and Northeastern Europe are analogues of East Antarctica, as all are tectonically stable regions. Therefore, we expect West and East Antarctica to have similar heat flux distributions to the analogous regions. Specifically, for the Western US, we find a spatial median of 68 $\mathrm{mW/m^2}$ with an IQR (25th percentile to 75th percentile) of about 20 $\mathrm{mW/m^2}$. Southwestern Europe has similar statistics but a slightly lower median and more variability. For the Eastern US, we find a spatial median of 51 $\mathrm{mW/m^2}$ with an IQR of about 9 $\mathrm{mW/m^2}$. Northeastern Europe has similar variability but a lower median of 45 $\mathrm{mW/m^2}$. Therefore, the statistical distributions of heat flux are quite similar both between the Western US and Southwestern Europe, and the Eastern US and Northeastern Europe. For East and West Antarctica, we expect a similar heat flux distribution to these stable and tectonic regions, respectively.

Zhang and Ritzwoller [39] find that the Decision Tree and Linear Regression models reasonably reproduce the statistical distribution of observations in both the US and Europe. **Fig. 5**cd here shows the predicted distributions in the tectonic and stable regions. The statistical distributions of the predicted values are within the observed distributions (difference of medians smaller than 5 $\mathrm{mW/m^2}$). The range of the predicted values, however, is smaller than that of the observations (IQR about 40% and 10% smaller for tectonic and stable regions, respectively). As discussed by Zhang and Ritzwoller [39], the predictions match the geographical distribution of heat flux values well but underpredict their variability. Therefore, we expect that our Antarctic heat flux estimates will have accurate medians and geographical patterns, but relatively low variability. This underestimation of variability is partially accounted for in our uncertainty estimation ϵ_γ (**section 3.4**).

For the purpose of comparison, we interpolate the heat flux estimates of Shen, Wiens, Lloyd, and Nyblade [1] and Martos et al. [2] onto the same grid as our heat flux estimates (50 km × 50 km) and smooth them using a Gaussian filter with a standard deviation of 50 km. We then summarize their spatial statistics in West and East Antarctica (**Fig. 5**ef) and compare with observations in the US and Europe.

In the tectonically stable East Antarctica, the estimates of Shen, Wiens, Lloyd, and Nyblade [1] and Martos et al. [2] are consistent with each other and with our estimates (**Fig. 5**f) in that their median values lie within 5 $\mathrm{mW/m^2}$ of each other. The statistical distribution of Martos et al. [2] extends to higher values than the distributions based on seismic structure. For example, the 95th percentile for Martos et al. [2] at the high end is approximately 70 $\mathrm{mW/m^2}$, whereas the predictions from the seismic proxies are lower than 62 $\mathrm{mW/m^2}$. Additionally, the predictions from Martos et al. [2] extend higher than the observations across Northeastern Europe and the Eastern US (95th percentile lower than 65 $\mathrm{mW/m^2}$).

For West Antarctica, our estimates are consistent with Shen, Wiens, Lloyd, and Nyblade [1] but systematically lower than Martos et al. [2], which has a heavy tail at high heat flux (**Fig. 5**e). This high tail is also missing from observations in tectonically active regions of the Western US and Southern Europe (**Fig. 5**a). For example, the 95th percentile of Martos et al. is about 135 $\mathrm{mW/m^2}$, in contrast with the 95th percentile of observations in the Southwestern Europe and Western US which are below 95 $\mathrm{mW/m^2}$.

If the estimates from Martos et al. are accurate in West Antarctica, then the Western US and Southwestern Europe on the whole are not good heat flux proxies for West Antarctica. We note that the heat flux observations in the Rio Grande Rift are much lower than the estimates from Martos et al., which we believe is a reasonable analogue for parts of West Antarctica.

In conclusion, we find that our heat flux estimates as well as those of Shen, Wiens, Lloyd, and Nyblade [1] in West and East Antarctica are consistent with the statistical distributions of observations in analogous tectonic and stable regions of the US and Europe. We believe that heat flux is overestimated in West Antarctica by Martos et al. [2], which disagrees with the distributions of heat flux observed in the US and Europe. This conclusion is further supported by the Curie depth estimates in the US from Bouligand, Glen, and Blakely [48]. They use a similar approach as Martos et al. [2] to estimate heat flux from Curie depth in the US, but they find that heat flux is systematically overestimated for regions with shallow Curie depths (e.g., Cascade Range, Basin and Range).

6 Conclusion

This work aims to estimate both the continental dichotomy and regional anomalies of heat flux across Antarctica with associated estimates of uncertainty in both. We produce heat flux estimates by transporting heat flux from the US and Europe based on seismic structure with a lateral resolution of about 100 km, using three Machine Learning models across a hierarchy of complexity. These are the Linear Regression, Decision Tree, and Random Forest models. These models have been validated within and cross-validated between the US and Europe in our previous study [39].

We find that Antarctic heat flux estimates are highly consistent between the Linear Regression and Decision Tree models. For simplicity, discussion in the following paragraphs is based on the Decision Tree model estimates.

For the large-scale east-west dichotomy problem, we estimate representative heat flux values of $64 \pm 7\,\mathrm{mW/m^2}$ (spatial mean $\pm$ standard deviation) and $53 \pm 3\,\mathrm{mW/m^2}$ in West and East Antarctica, respectively. We note that we probably underestimate spatial variability particularly in West Antarctica. In East Antarctica, these statistics are consistent with both the previous seismically-based estimate by Shen, Wiens, Lloyd, and Nyblade [1] and observations in the tectonically stable regions of the Eastern US and Northeastern Europe. In West Antarctica, our estimates are systematically lower than the magnetically-based estimate by Martos et al. [2], which is also higher than observations in the tectonically recently deformed Western US and Southern Europe. We hypothesize that Martos et al. [2] overestimates heat flux in West Antarctica.

For the regional-scale anomaly problem, we identify the same robust features from all three

Machine Learning models. High heat flux occurs in the western Transantarctic Mountains and Marie Byrd Land ($80\pm20\,\mathrm{mW/m^2}$). These high anomalies are associated with slow uppermost mantle and crustal V_S. Low heat flux happens in Victoria Land, the Wilkes Subglacial Basin, the Vostok Subglacial Highland, and south of Maud Subglacial Basin ($50\pm7\,\mathrm{mW/m^2}$). These low anomalies are associated with slow uppermost mantle V_S and thick crust. These associations are uniquely illuminated by the Decision Tree model.

To estimate the uncertainties associated with our heat flux estimates, we identify four main sources of uncertainty. We estimate systematic errors of both a constant shift in the continental average ($2.5\,\mathrm{mW/m^2}$) and a variability (higher highs, lower lows) of 25% from the continental average, along with an average local random error of about 13 $\mathrm{mW/m^2}$ in West Antarctica and 10 $\mathrm{mW/m^2}$ in East Antarctica. These uncertainties are caused by the differences in the heat flux observations and Machine Learning models between the US and Europe, and uncertainties in seismic structure information.

Heat flux estimation in Antarctica can be improved further by improving the number and quality of existing heat flux observations outside Antarctica [49] and by producing better images of seismic structure in Antarctica and outside Antarctica where heat flux observations are available. Improvement is also expected by combining seismic structure with other proxies, such as magnetic Curie depth and surface topography [e.g., 26, 28, 29]. However, all proxies need to be validated outside Antarctica, such as in the US and Europe as discussed by Zhang and Ritzwoller [39]. This validation is crucial for resolving the inconsistencies between heat flux estimates for Antarctica based on different proxies, such as those between Martos et al. [2] and this study in West Antarctica.

Resolving existing inconsistencies between different heat flux proxies would improve the reliability of estimates of heat flux beneath Antarctica, which can better constrain the subglacial thermal boundary conditions of the Antarctic ice sheet. This would lead to more accurate dynamic modeling of the Antarctic ice sheet both to illuminate its evolution in the past and to predict the extent of stability in the future. The stability of the Antarctic ice sheet will affect its contribution to future sea level change.

Figures

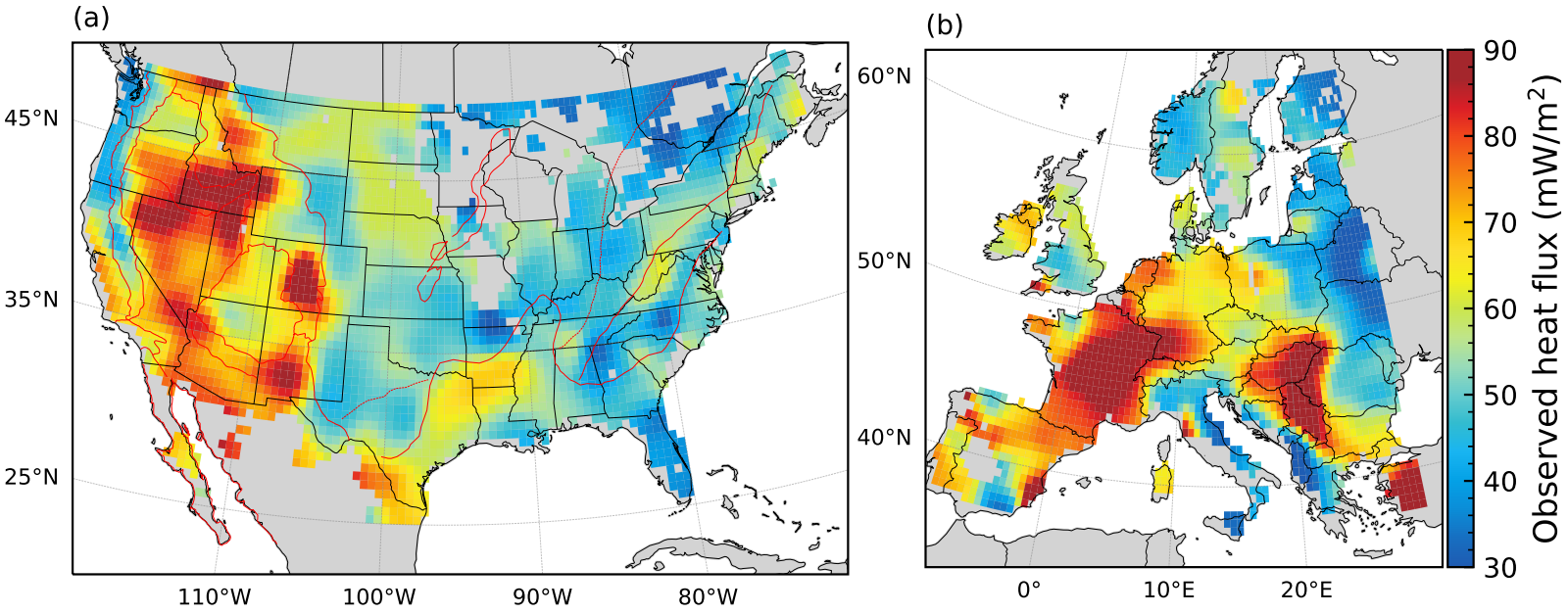

Figure 1: **Heat flux observations.** (a) Heat flux observations after quality control and smoothing, plotted in the US. Red lines denote geological provinces [50]. Gaps in the Midwestern US are caused by lack of observations. (b) Similar to (a) except in Europe. These data are based on Lucazeau [40] and Blackwell et al. [41].

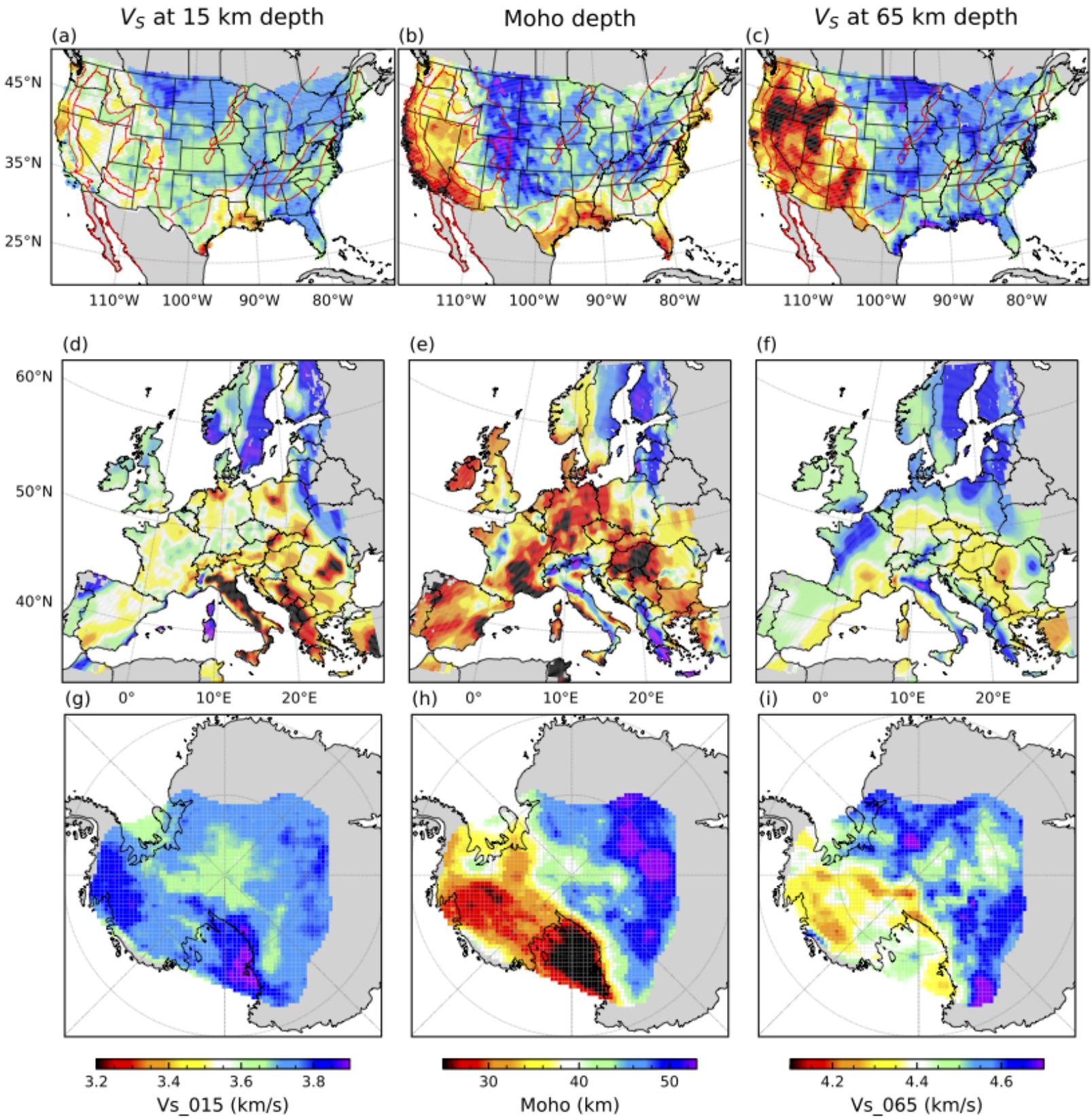

Figure 2: **Seismic structure.** (a)–(c) In the US, seismic structure plotted for (a) the V_S at 15 km depth, (b) Moho depth, (c) V_S at 65 km depth from Shen and Ritzwoller [35]. (d)–(f) Similar to (a)–(c) except in Europe from Lu, Stehly, and Paul [36]. (g)–(i) Similar to (a)–(c) except in Antarctica from Shen et al. [37]. The gap in East Antarctica is caused by the lack of seismic station coverage there.

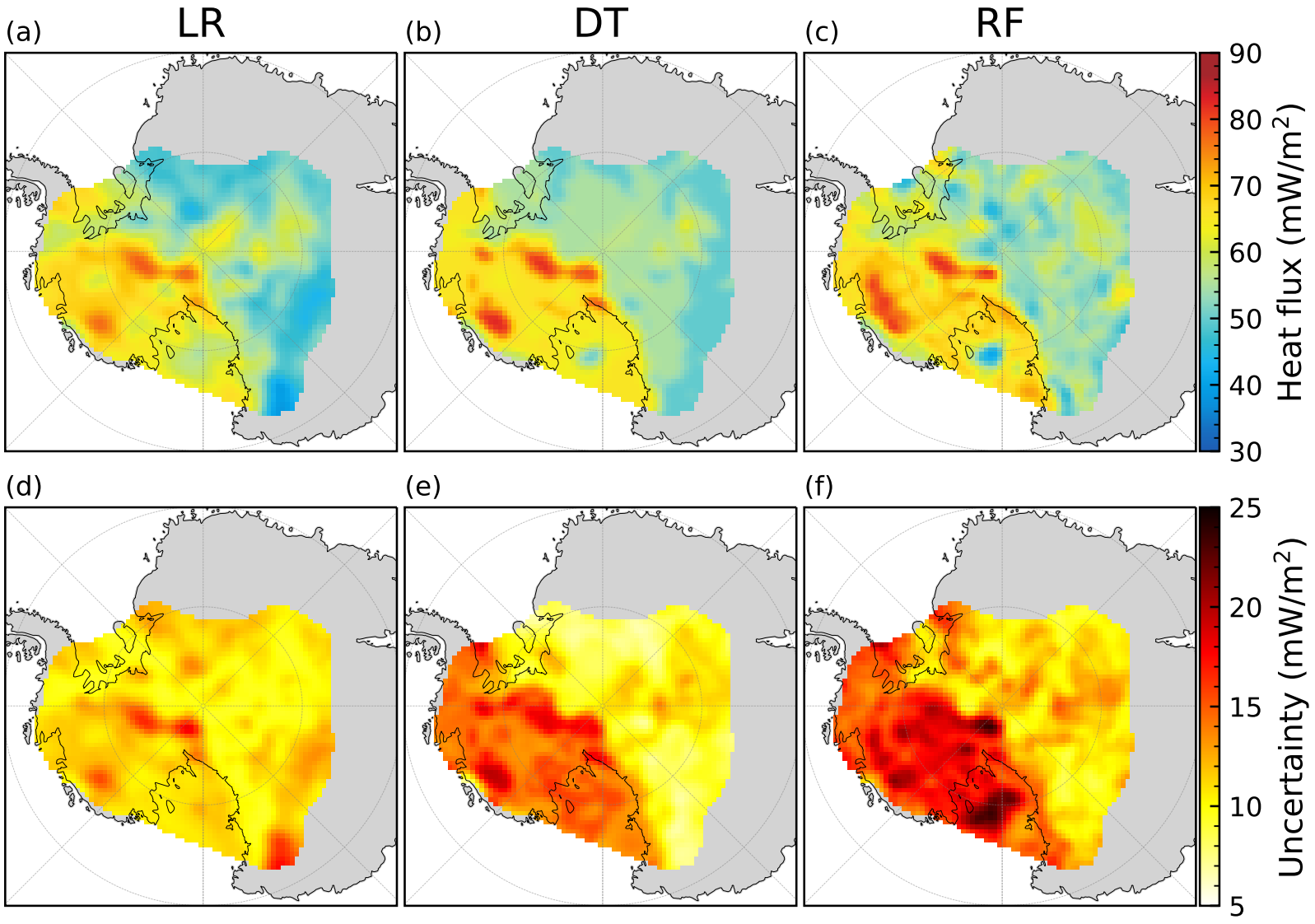

Figure 3: **Heat flux predictions across Antarctica.** (a)–(c) Heat flux estimates across Antarctica from (a) the Linear Regression (LR), (b) Decision Tree (DT), and (c) Random Forest (RF) models. (d)–(f) Uncertainties associated with (a)–(c), respectively.

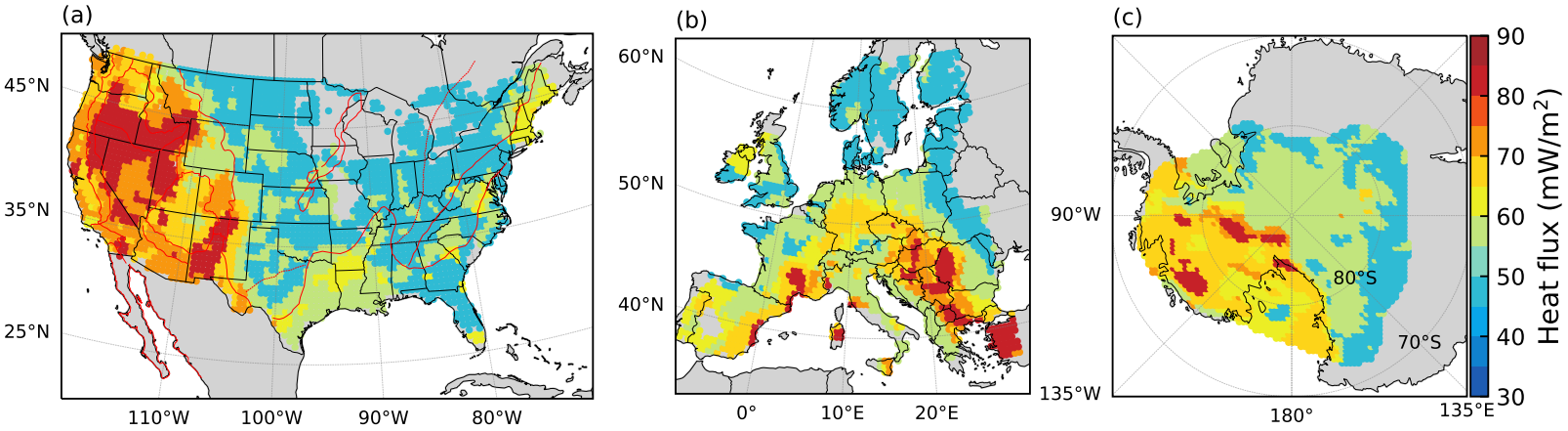

Figure 4: **Identifying regions in the US and Europe that transport heat flux to Antarctica.** In (a) the US, (b) Europe, and (c) Antarctica, predicted heat flux from the Decision Tree model is plotted. These maps are presented to identify regions in the US and Europe that transport heat flux predictions to Antarctica.

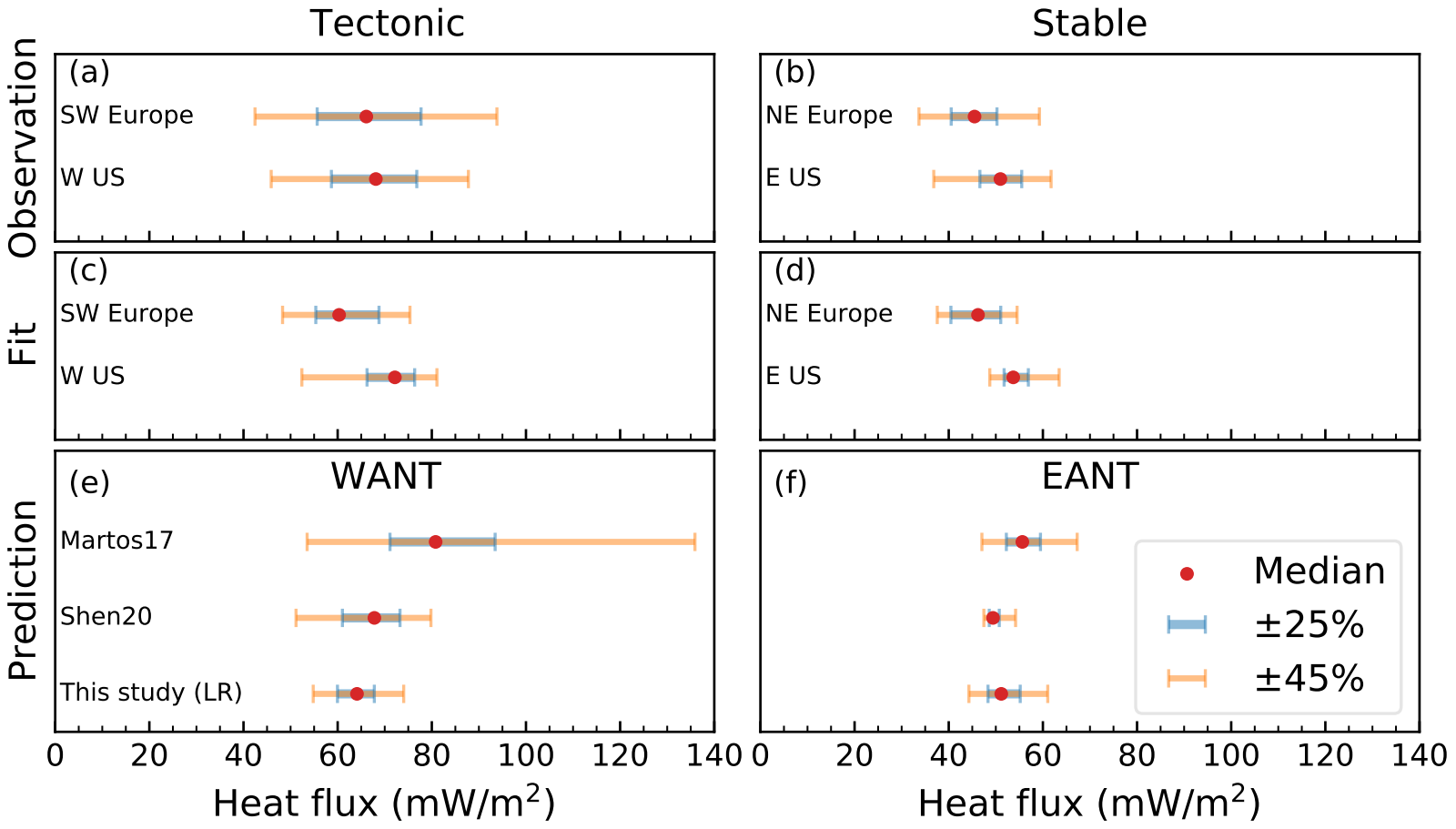

Figure 5: **Comparison with previous studies.** (a) & (b) Statistical summaries of heat flux observations in the US and Europe are shown for (a) Western US (W US) and Southwestern Europe (SW Europe), and (b) Eastern US (E US) and Northeastern Europe (NE Europe). Red circles denote the median of a region, while blue and orange bars denote ±25% from the median (25th percentile to 75th percentile) and ±45% from the median (5th percentile to 95th percentile), respectively. (c) & (d) Similar to (a) & (b) but from heat flux estimates based on the Linear Regression model trained using the US and Europe data. (e) & (f) Similar to (a) & (b) but for heat flux estimates in Antarctica (ANT) including (a) West Antarctica (WANT) and (b) East Antarctica (EANT). This study uses three Machine Learning models but only the Linear Regression (LR) estimates are shown for simplicity. Martos17 = Martos et al. [2], Shen20 = Shen, Wiens, Lloyd, and Nyblade [1].

CRediT authorship contribution statement

Shane Zhang: Data curation; Formal analysis; Investigation; Methodology; Software; Visualization; Writing - original draft; Writing - review & editing. **Michael H. Ritzwoller:** Conceptualization; Funding acquisition; Methodology; Project administration; Resources; Supervision; Writing - review & editing.

Data Availability

We implement the Machine Learning models with `scikit-learn` [51]. Francis Lucazeau provided the NGHF data [40], SMU Geothermal Lab maintains the SMU Node of the National Geothermal Data System [`http://geothermal.smu.edu/gtda`; 41], Weisen Shen provided the US [35] and Antarctica [37] seismic structure, and Yang Lu provided the European seismic structure [36]. Upon acceptance of the manuscript, our heat flux estimates will be made publicly available.

Funding

S.Z. were supported by a CIRES Graduate Student Research Award. M.H.R. and S.Z. were supported by NSF grant EAR-1943112 at the University of Colorado Boulder.

Acknowledgements

We acknowledge helpful discussions with Robert Anderson, Shijie Zhong, Kyle Goodrick, and Derek Mease. We thank Francis Lucazeau, the SMU Geothermal Lab, Weisen Shen, and Yang Lu for sharing the data identified in the Data Availability section.

Appendix A Decision rules

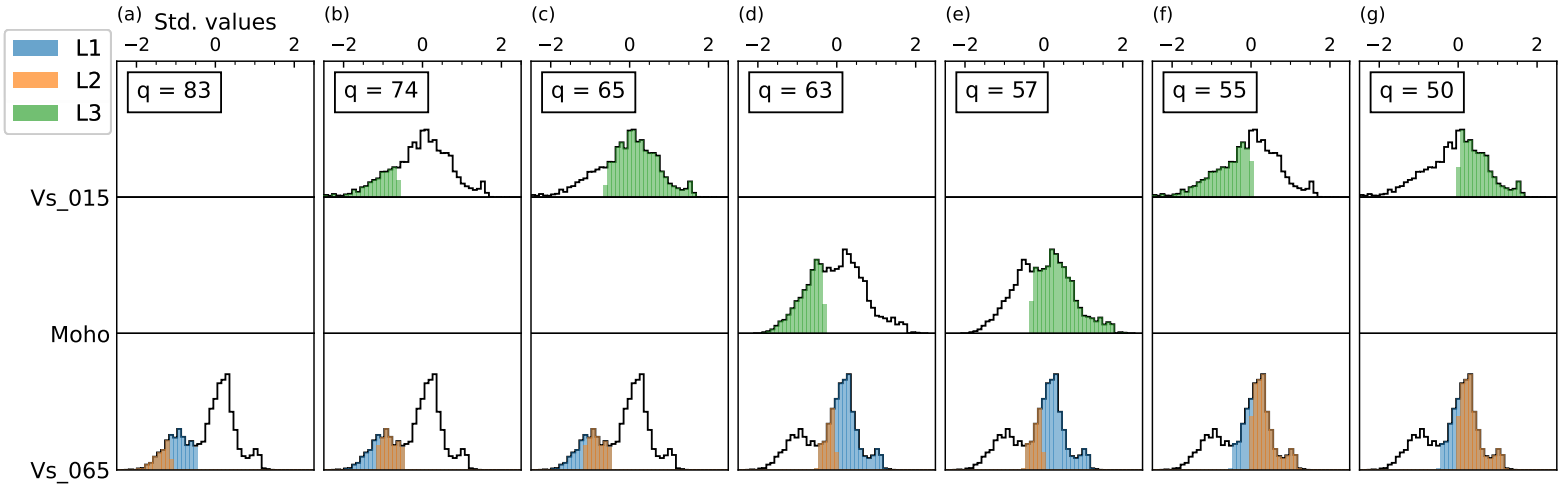

Figure A.1: **Decision rules obatined from the Decision Tree model.** Each column represents a decision rule, ordered by decreasing heat flux predictions q from left to right ($83\,\mathrm{mW/m^2}$ to $50\,\mathrm{mW/m^2}$). Each row denotes one of the three seismic structural variables and the variables are increasing with depth from top to bottom (V_S at 15 km depth, Moho depth, and V_S at 65 km depth). The full statistical distributions of the variables are shown as black histograms, where the values have been standardized (**eq.** (1)). For each decision rule (column), the variables are successively split by certain threshold values, with the order of splitting color-coded in blue, orange, and green for increasing levels of $L = 1, 2, 3$. Note that the distributions are often split at valleys or peaks, which tend to correlate with geological boundaries.

Appendix B Uncertainty estimation

We identify and model the effect of five sources of uncertainty: (1) & (2) differences in the (1) median and (2) variability of the statistical distributions of heat flux observations between the US and Europe; (3) differences in the estimates from the Machine Learning models trained in the US and Europe; (4) errors in the seismic structure information in Antarctica; and (5) errors in heat flux observations in the US and Europe. We denote uncertainties from these five sources of error as $\epsilon_\mu, \epsilon_\gamma, \epsilon_m, \epsilon_v$ and ϵ_q, respectively.

(1) The medians of the statistical distribution of heat flux observations between the US and Europe are different. The median μ of heat flux in the US and Europe are $55\,\mathrm{mW/m^2}$ and $60\,\mathrm{mW/m^2}$, respectively. This means that compared to the US heat flux observations, the European data are higher on average. This difference can change the absolute amplitudes of heat flux estimates transported to Antarctica but not the geographic patterns. Specifically, for Antarctic estimates, the median μ can shift by about $\pm 2.5\,\mathrm{mW/m^2}$, which we denote as $\epsilon_\mu \approx 2.5\,\mathrm{mW/m^2}$ (**Figs B.1** and **B.2** first row).

(2) The variability of the statistical distributions of heat flux observations between the US and Europe is different. The IQR (interquartile range; **eq.** (1)) γ of heat flux in the US and Europe are $15\,\mathrm{mW/m^2}$ and $25\,\mathrm{mW/m^2}$, respectively. This means that compared to the US heat flux observations, the European data are more spatially variable. This difference can change the absolute amplitudes of heat flux estimates transported to Antarctica but not the geographic patterns. Specifically, for Antarctic estimates q, the amplitude of variation γ can oscillate around the median μ by about 25%, which we denote the absolute value of this oscillation as $\epsilon_\gamma \approx 0.25|q-\mu|$. For example, if the median $\mu = 60\,\mathrm{mW/m^2}$, then an estimate $q = 80\,\mathrm{mW/m^2}$ has an uncertainty ϵ_γ of $5\,\mathrm{mW/m^2}$ (**Figs B.1** and **B.2** second row).

(3) The Machine Learning models trained in the US and Europe are different. This difference means that similar seismic structure between the US and Europe can predict distinct heat flux values, even after accounting for the difference in the heat flux distributions between the two continents (ϵ_μ and ϵ_γ). To quantify how this difference affects Antarctic predictions, we first undo the standardization with a common median μ and IQR γ for the standardized heat flux observations in the US and Europe ($\mu = 57\,\mathrm{mW/m^2}, \gamma = 19\,\mathrm{mW/m^2}$). Then we train the Machine Learning models with different weights on the US versus European data. We find that weighting either the US or European data twice more does not change heat flux predictions significantly (difference Δ about $\pm 1\,\mathrm{mW/m^2}$). However, using either the US or European data alone can produce differences Δ as large as $\pm 10\,\mathrm{mW/m^2}$. Therefore, we use half the absolute values of this difference from using either the US or European data alone Δ as the uncertainty: $\epsilon_m = |\Delta|/2$. Typical values of ϵ_m are about $5\,\mathrm{mW/m^2}$ (**Figs B.1** and **B.2** third row).

(4) Seismic structure information in Antarctica is presented with associated uncertainty estimates. These errors can arise from biases in seismic measurements and non-uniqueness in seismic inversions. Shen et al. [37] estimate uncertainties for the V_S at 15 km, V_S at 65 km, and Moho depth of about 1% (0.05 km/s), 2% (0.1 km/s), and 10% (4 km), respectively. For the Decision Tree and Random Forest models, we first randomly perturb the

seismic variables assuming Gaussian distributions with these uncertainties as standard deviations. Then we compute the standard deviation of predictions from 1000 such perturbations and use it as a prediction uncertainty. For the Linear Regression models, the perturbation is not needed and the uncertainty can be linearly propagated from seismic variable uncertainty. We estimate this uncertainty to be about $6.5\,\mathrm{mW/m^2}$ (**Figs B.1** and **B.2** fourth row).

(5) Heat flux observations in the US and Europe also have errors, which can result from local or non-steady state processes such as paleoclimate variations, sedimentation and erosion, seismicity, and ground water or magma convection [52]. Unfortunately, most heat flux observations do not have associated quality information such as measurement errors and site characterization. Therefore, we use the spatial variability of heat flux (MAD) as a proxy for its uncertainty. In both the US and Europe, the spatial MAD values of heat flux observations within a 100 km radius are about $10\,\mathrm{mW/m^2}$. For the Linear Regression model, this propagates to an error of about $0.3\,\mathrm{mW/m^2}$ in heat flux estimates: $\epsilon_q \approx 0.3\,\mathrm{mW/m^2}$. The model has a reduced chi-squared misfit of about 0.9. This uncertainty is also small for the Decision Tree and Random Forest models. This is because these models make predictions by averaging a large number of heat flux observations (typically > 100).

The uncertainties are combined according to **eq.** (2) and are shown in **Fig. 3**d–f and **Fig. B.2**m–o.

We compare predictions from the three Machine Learning models and find their differences are smaller than uncertainties (MAD about $4\,\mathrm{mW/m^2}$; **Fig. B.3**). Moreover, we find that the Linear Regression and Decision Tree predictions are the most similar, while the Linear Regression and Random Forest predictions are the most different.

We expect, however, this uncertainty ϵ to be no smaller than the misfit of the Machine Learning models against the validation datasets in the US and Europe. The misfit composes multiple errors including both those listed above and others such as model inaccuracy. For example, the Linear Regression model cannot be highly accurate if the relationship between heat flux and seismic structure is strongly nonlinear. Thus, our most optimistic expectation about errors is from the validation within the US, which is better than that in Europe [39]. These metrics are $r^2 \approx 0.6$ (coefficient of determination which measures normalized overall misfit), RMSE $\approx 8\,\mathrm{mW/m^2}$ (Root Mean Squared Error which measures overall misfit), $\rho = 0.9$ (Pearson's correlation coefficient which measures geographic coherence). On the other hand, the errors can turn out smaller than those from transporting between the US and Europe ($r^2 \approx 0.4, \mathrm{RMSE} = 10\,\mathrm{mW/m^2}, \rho \approx 0.7$ from Europe to the US, and being worse vice versa). This is because the seismic structure information in Antarctica from Shen et al. [37] is constructed more similarly to that in the US from Shen and Ritzwoller [35] than that in Europe from Lu, Stehly, and Paul [36], *ceteris paribus*.

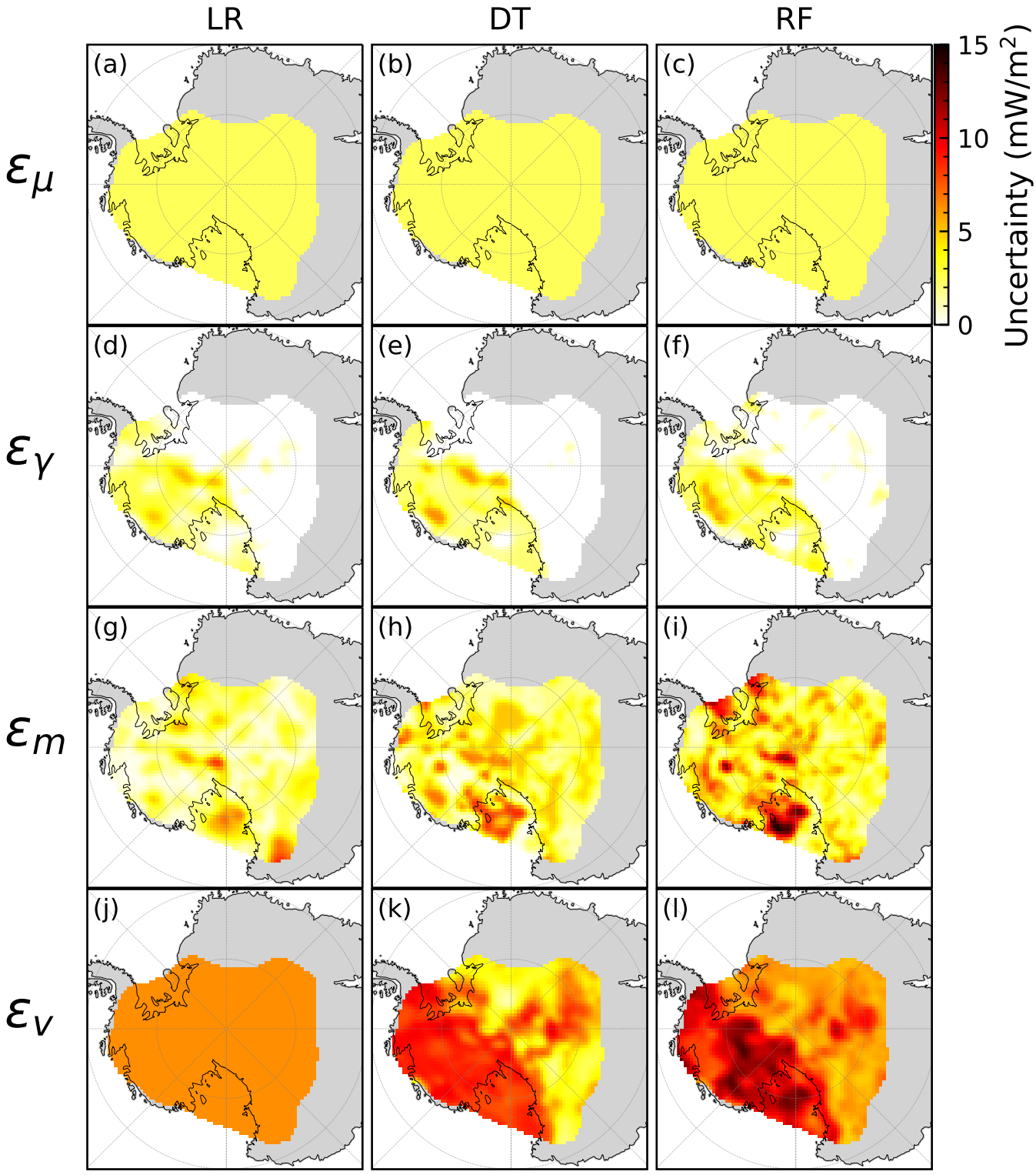

Figure B.1: **Sources of uncertainties.** (a)–(c) The uncertainty ϵ_μ is plotted for (a) the Linear Regression (LR), (b) Decision Tree (DT), and (c) Random Forest (RF) models. (d)–(l) Similar to (a)–(c) except for the uncertainty (d)–(f) ϵ_γ, (g)–(i) ϵ_m, (j)–(l) ϵ_v. The combined uncertainties are shown in **Fig. 3**d–f.

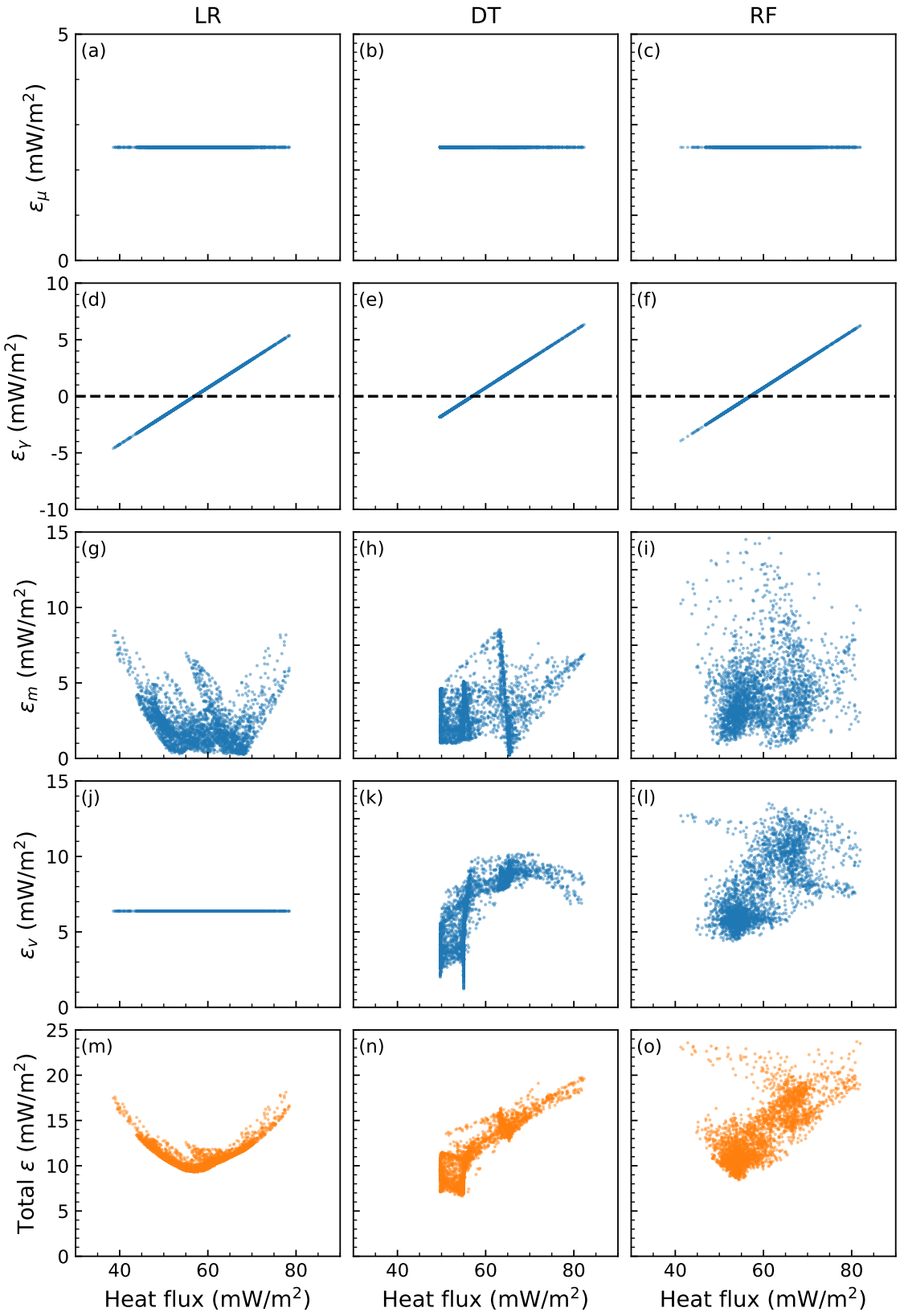

Figure B.2: **Uncertainty versus heat flux.** (a)–(l) Similar to **Fig. B.1**a–l except that the uncertainties are plotted as a function of heat flux predictions. (m)–(o) The combined uncertainties are shown (**Fig. 3**d–f).

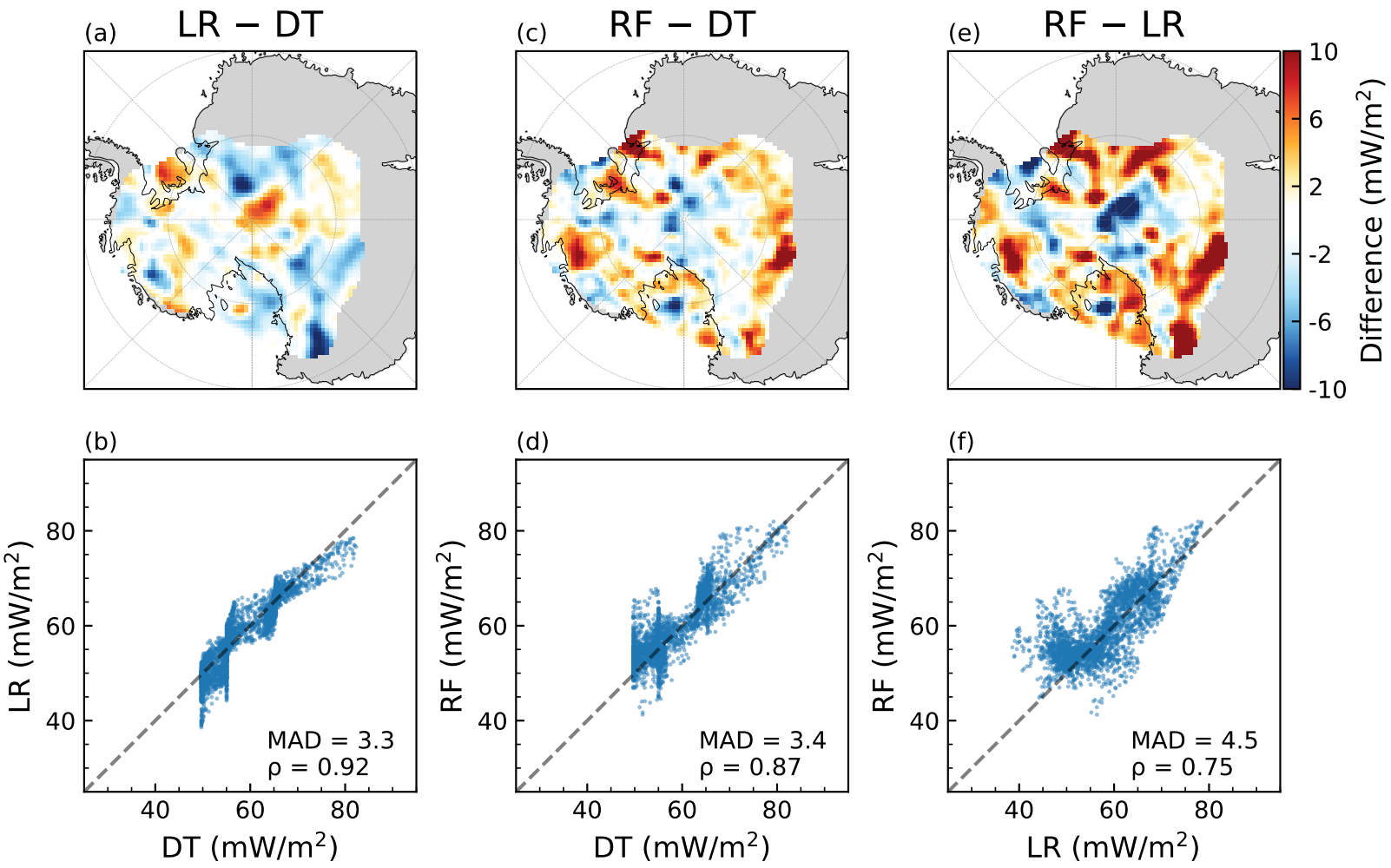

Figure B.3: **Differences between predictions from the three Machine Learning models.** (a) Difference between predictions from the Linear Regression (LR) and Decision Tree (DT) models. (b) Predictions from LR versus DT. The MAD (median absolute deviation) has a unit of mW/m^2. The ρ denotes the linear correlation coefficient. (c) & (d) Similar to (a) & (b) except between Random Forest (RF) and DT. (e) & (f) Similar to (a) & (b) except between RF and LR.

References

[1]W. Shen, D. Wiens, A. Lloyd, and A. Nyblade, "A Geothermal Heat Flux Map of Antarctica Empirically Constrained by Seismic Structure", Geophysical Research Letters **47**, e2020GL086955 (2020).

[2]Y. M. Martos, M. Catalán, T. A. Jordan, A. Golynsky, D. Golynsky, G. Eagles, and D. G. Vaughan, "Heat Flux Distribution of Antarctica Unveiled", Geophysical Research Letters **44**, 11, 417–11, 426 (2017).

[3]M. J. Siegert and J. A. Dowdeswell, "Spatial Variations in Heat at the Base of the Antarctic Ice Sheet from Analysis of the Thermal Regime above Subglacial Lakes", Journal of Glaciology **42**, 501–509 (1996/ed).

[4]D. Pollard, R. M. DeConto, and A. A. Nyblade, "Sensitivity of Cenozoic Antarctic Ice Sheet Variations to Geothermal Heat Flux", Global and Planetary Change **49**, 63–74 (2005).

[5]M. Llubes, C. Lanseau, and F. Rémy, "Relations between Basal Condition, Subglacial Hydrological Networks and Geothermal Flux in Antarctica", Earth and Planetary Science Letters **241**, 655–662 (2006).

[6]F. Pattyn, "Antarctic Subglacial Conditions Inferred from a Hybrid Ice Sheet/Ice Stream Model", Earth and Planetary Science Letters **295**, 451–461 (2010).

[7]J. Lai and A. M. Anders, "Tectonic Controls on Rates and Spatial Patterns of Glacial Erosion through Geothermal Heat Flux", Earth and Planetary Science Letters **543**, 116348 (2020).

[8]C. B. Begeman, S. M. Tulaczyk, and A. T. Fisher, "Spatially Variable Geothermal Heat Flux in West Antarctica: Evidence and Implications", Geophysical Research Letters **44**, 9823–9832 (2017).

[9]F. S. McCormack, J. L. Roberts, C. F. Dow, T. Stål, J. A. Halpin, A. M. Reading, and M. J. Siegert, "Fine-Scale Geothermal Heat Flow in Antarctica Can Increase Simulated Subglacial Melt Estimates", Geophysical Research Letters **49**, e2022GL098539 (2022).

[10]E. Larour, M. Morlighem, H. Seroussi, J. Schiermeier, and E. Rignot, "Ice Flow Sensitivity to Geothermal Heat Flux of Pine Island Glacier, Antarctica", Journal of Geophysical Research: Earth Surface **117**, 10.1029/2012JF002371 (2012).

[11]B. V. Liefferinge and F. Pattyn, "Using Ice-Flow Models to Evaluate Potential Sites of Million Year-Old Ice in Antarctica", Climate of the Past **9**, 2335–2345 (2013).

[12]M. L. Pittard, B. K. Galton-Fenzi, J. L. Roberts, and C. S. Watson, "Organization of Ice Flow by Localized Regions of Elevated Geothermal Heat Flux", Geophysical Research Letters **43**, 3342–3350 (2016).

[13]M. L. Pittard, J. L. Roberts, B. K. Galton-Fenzi, and C. S. Watson, "Sensitivity of the Lambert-Amery Glacial System to Geothermal Heat Flux", Annals of Glaciology **57**, 56–68 (2016).

[14]S. Smith-Johnsen, B. de Fleurian, and K. H. Nisancioglu, "The Role of Subglacial Hydrology in Ice Streams with Elevated Geothermal Heat Flux", Journal of Glaciology, 1–10 (2020).

[15]E. J. Dawson, D. M. Schroeder, W. Chu, E. Mantelli, and H. Seroussi, "Ice Mass Loss Sensitivity to the Antarctic Ice Sheet Basal Thermal State", Nature Communications **13**, 4957 (2022).

[16]T. L. Noble, E. J. Rohling, A. R. A. Aitken, H. C. Bostock, Z. Chase, N. Gomez, L. M. Jong, M. A. King, A. N. Mackintosh, F. S. McCormack, R. M. McKay, L. Menviel, S. J. Phipps, M. E. Weber, C. J. Fogwill, B. Gayen, N. R. Golledge, D. E. Gwyther, A. M. C. Hogg, Y. M. Martos, B. Pena-Molino, J. Roberts, T. van de Flierdt, and T. Williams, "The Sensitivity of the Antarctic Ice Sheet to a Changing Climate: Past, Present and Future", Reviews of Geophysics **58**, e2019RG000663 (2020).

[17]A. Burton-Johnson, R. Dziadek, and C. Martin, "Geothermal Heat Flow in Antarctica: Current and Future Directions", The Cryosphere **14**, 3843–3873 (2020).

[18]P. Talalay, Y. Li, L. Augustin, G. D. Clow, J. Hong, E. Lefebvre, A. Markov, H. Motoyama, and C. Ritz, "Geothermal Heat Flux from Measured Temperature Profiles in Deep Ice Boreholes in Antarctica", The Cryosphere **14**, 4021–4037 (2020).

[19]N. M. Shapiro and M. H. Ritzwoller, "Thermodynamic Constraints on Seismic Inversions", Geophysical Journal International **157**, 1175–1188 (2004).

[20]J. W. Goodge, "Crustal Heat Production and Estimate of Terrestrial Heat Flow in Central East Antarctica, with Implications for Thermal Input to the East Antarctic Ice Sheet", Cryosphere **12**, 491–504 (2018).

[21]A. Pollett, D. Hasterok, T. Raimondo, J. A. Halpin, M. Hand, B. Bendall, and S. McLaren, "Heat Flow in Southern Australia and Connections With East Antarctica", Geochemistry, Geophysics, Geosystems **20**, 5352–5370 (2019).

[22]S. N. P. Guimarães, F. P. Vieira, and V. M. Hamza, "Heat Flow Variations in the Antarctic Continent", International Journal of Terrestrial Heat Flow and Applied Geothermics **3**, 1–10 (2020).

[23]R. Dziadek, F. Ferraccioli, and K. Gohl, "High Geothermal Heat Flow beneath Thwaites Glacier in West Antarctica Inferred from Aeromagnetic Data", Communications Earth & Environment **2**, 1–6 (2021).

[24]M. Lösing and J. Ebbing, "Predicting Geothermal Heat Flow in Antarctica With a Machine Learning Approach", Journal of Geophysical Research: Solid Earth **126**, e2020JB021499 (2021).

[25]T. Stål, A. M. Reading, J. A. Halpin, and J. M. Whittaker, "Antarctic Geothermal Heat Flow Model: Aq1", Geochemistry, Geophysics, Geosystems **22**, e2020GC009428 (2021).

[26]I. M. Artemieva, "Antarctica Ice Sheet Basal Melting Enhanced by High Mantle Heat", Earth-Science Reviews **226**, 103954 (2022).

[27]C. Haeger, A. G. Petrunin, and M. K. Kaban, "Geothermal Heat Flow and Thermal Structure of the Antarctic Lithosphere", Geochemistry, Geophysics, Geosystems **23**, e2022GC010501 (2022).

[28]C. Fox Maule, M. E. Purucker, N. Olsen, and K. Mosegaard, "Heat Flux Anomalies in Antarctica Revealed by Satellite Magnetic Data", Science **309**, 464–467 (2005).

[29]B. Goutorbe, J. Poort, F. Lucazeau, and S. Raillard, "Global Heat Flow Trends Resolved from Multiple Geological and Geophysical Proxies", Geophysical Journal International **187**, 1405–1419 (2011).

[30]D. M. Schroeder, D. D. Blankenship, D. A. Young, and E. Quartini, "Evidence for Elevated and Spatially Variable Geothermal Flux beneath the West Antarctic Ice Sheet", Proceedings of the National Academy of Sciences **111**, 9070–9072 (2014).

[31]M. An, D. A. Wiens, Y. Zhao, M. Feng, A. Nyblade, M. Kanao, Y. Li, A. Maggi, and J.-J. Lévêque, "Temperature, Lithosphere-Asthenosphere Boundary, and Heat Flux beneath the Antarctic Plate Inferred from Seismic Velocities", Journal of Geophysical Research: Solid Earth **120**, 8720–8742 (2015).

[32]A. Burton-Johnson, J. A. Halpin, J. M. Whittaker, F. S. Graham, and S. J. Watson, "A New Heat Flux Model for the Antarctic Peninsula Incorporating Spatially Variable Upper Crustal Radiogenic Heat Production", Geophysical Research Letters **44**, 5436–5446 (2017).

[33]O. Passalacqua, C. Ritz, F. Parrenin, S. Urbini, and M. Frezzotti, "Geothermal Flux and Basal Melt Rate in the Dome C Region Inferred from Radar Reflectivity and Heat Modelling", The Cryosphere **11**, 2231–2246 (2017).

[34]T. A. Jordan, C. Martin, F. Ferraccioli, K. Matsuoka, H. Corr, R. Forsberg, A. Olesen, and M. Siegert, "Anomalously High Geothermal Flux near the South Pole", Scientific Reports **8**, 16785 (2018).

[35]W. Shen and M. H. Ritzwoller, "Crustal and Uppermost Mantle Structure beneath the United States", Journal of Geophysical Research: Solid Earth **121**, 4306–4342 (2016).

[36]Y. Lu, L. Stehly, and A. Paul, "High-Resolution Surface Wave Tomography of the European Crust and Uppermost Mantle from Ambient Seismic Noise", Geophysical Journal International **214**, 1136–1150 (2018).

[37]W. Shen, D. A. Wiens, S. Anandakrishnan, R. C. Aster, P. Gerstoft, P. D. Bromirski, S. E. Hansen, I. W. D. Dalziel, D. S. Heeszel, A. D. Huerta, A. A. Nyblade, R. Stephen, T. J. Wilson, and J. P. Winberry, "The Crust and Upper Mantle Structure of Central and West Antarctica From Bayesian Inversion of Rayleigh Wave and Receiver Functions", Journal of Geophysical Research: Solid Earth **123**, 7824–7849 (2018).

[38]A. J. Lloyd, D. A. Wiens, H. Zhu, J. Tromp, A. A. Nyblade, R. C. Aster, S. E. Hansen, I. W. D. Dalziel, T. Wilson, E. R. Ivins, and J. P. O'Donnell, "Seismic Structure of the Antarctic Upper Mantle Imaged with Adjoint Tomography", Journal of Geophysical Research: Solid Earth **125**, 10.1029/2019JB017823 (2020).

[39]S. Zhang and M. Ritzwoller, "Applying Machine Learning to Characterize and Transport the Relationship Between Seismic Structure and Surface Heat Flux", Geophysical Journal International (submitted), 10.31223/X5HM21 (2023).

[40]F. Lucazeau, "Analysis and Mapping of an Updated Terrestrial Heat Flow Data Set", Geochemistry, Geophysics, Geosystems **20**, 4001–4024 (2019).

[41]D. Blackwell, M. Richards, Z. Frone, J. Batir, A. Ruzo, R. Dingwall, and M. Williams, "Temperature-At-Depth Maps for the Conterminous U. S. and Geothermal Resource Estimates", GRC Transactions, 7 (2013).

[42]N. M. Shapiro and M. H. Ritzwoller, "Monte-Carlo Inversion for a Global Shear-Velocity Model of the Crust and Upper Mantle", Geophysical Journal International **151**, 88–105 (2002).

[43]N. M. Shapiro, M. Campillo, L. Stehly, and M. H. Ritzwoller, "High-Resolution Surface-Wave Tomography from Ambient Seismic Noise", Science **307**, 1615–1618 (2005).

[44]K. G. Sabra, P. Gerstoft, P. Roux, W. A. Kuperman, and M. C. Fehler, "Surface Wave Tomography from Microseisms in Southern California", Geophysical Research Letters **32**, L14311 (2005).

[45]A. Tarantola, *Inverse Problem Theory and Methods for Model Parameter Estimation*, Vol. 89 (Society for Industrial and Applied Mathematics, Philadelphia, PA, 2005), 342 pp.

[46]L. Breiman, J. H. Friedman, R. A. Olshen, and C. J. Stone, *Classification and Regression Trees* (Routledge, 2017).

[47]L. Breiman, "Random Forests", Machine Learning **45**, 5–32 (2001).

[48]C. Bouligand, J. M. G. Glen, and R. J. Blakely, "Mapping Curie Temperature Depth in the Western United States with a Fractal Model for Crustal Magnetization", Journal of Geophysical Research: Solid Earth **114**, 10.1029/2009JB006494 (2009).

[49]S. Fuchs, G. Beardsmore, P. Chiozzi, O. M. Espinoza-Ojeda, G. Gola, W. Gosnold, R. Harris, S. Jennings, S. Liu, R. Negrete-Aranda, F. Neumann, B. Norden, J. Poort, D. Rajver, L. Ray, M. Richards, J. D. Smith, A. Tanaka, and M. Verdoya, "A New Database Structure for the IHFC Global Heat Flow Database", International Journal of Terrestrial Heat Flow and Applied Geothermics **4**, 1–14 (2021).

[50]N. M. Fenneman and D. W. Johnson, "Physical Divisions of the United States", Reston, VA: US Geological Survey (1946).

[51]F. Pedregosa, G. Varoquaux, A. Gramfort, V. Michel, B. Thirion, O. Grisel, M. Blondel, P. Prettenhofer, R. Weiss, V. Dubourg, J. Vanderplas, A. Passos, D. Cournapeau, M. Brucher, M. Perrot, and É. Duchesnay, "Scikit-Learn: Machine Learning in Python", Journal of Machine Learning Research **12**, 2825–2830 (2011).

[52]W. G. Powell, D. S. Chapman, N. Balling, and A. E. Beck, "Continental Heat-Flow Density", Handbook of Terrestrial Heat-Flow Density Determination: with Guidelines and Recommendations of the International Heat-Flow Commission, 167–222 (1988).